Re-evaluation of the Bond Length–Bond Strength Rule: The Stronger Bond Is not Always the Shorter Bond

Elfi Kraka,* Dani Setiawan, and Dieter Cremer

A set of 42 molecules with N-F, O-F, N-Cl, P-F, and As-F bonds has been investigated in the search for potential bond anomalies, which lead to reverse bond length–bond strength (BLBS) relationships. The intrinsic strength of each bond investigated has been determined by the local stretching force constant obtained at the CCSD(T)/aug-cc-pVTZ level of theory. N-F or O-F bond anomalies were found for fluoro amine radicals, fluoro amines, and fluoro oxides, respectively. A rationale for the deviation from the normal Badger-type inverse BLBS relation is given and it is shown that electron withdrawal accompanied by strong orbital contraction and bond shortening is one of the prerequisites for a bond anomaly. In the case of short electron-rich bonds such as N-F or O-F, anomeric delocalization of lone pair electrons in connection with lone pair repulsion are decisive whether a bond anomaly can be observed. This is quantitatively assessed with the help of the CCSD(T) local stretching force constants, CCSD(T) charge distributions, and G4 bond dissociation energies. Bond anomalies are not found for fluoro phosphines and fluoro arsines because the bond weakening effects are no longer decisive. © 2015 Wiley Periodicals, Inc.

Introduction

One of the early discoveries of vibrational spectroscopy revealed that for diatomics an *inverse* power relationship between force constant k and bond length r exists. This so-called *Badger Rule*[1,2] was the basis for the tenet relating shorter bonds to stronger bonds. Numerous attempts aiming at a polyatomic generalization of the Badger rule have been published in the last 80 years[3,4] and, even though only of limited success, they have cemented the belief of chemists in the use of bond lengths as useful bond strength indicators. In the last three decades, a few observations that suggest a *reverse* bond length-bond strength (BLBS) relationship were published without attracting much attention. For example, reverse relationships were found for the N-F bonds in the fluoro amines $HnNF_{3-n}$ and methyl fluoro amines $(CH3)_nNF_{3-n}$ with ($n = 0–2$),[5–12] the fluorine bonds in substituted ethane homologues,[13–15] the O-F bonds in HOF, OF_2, and FNO_2[16–20] or the S-F bonds in the SF_2 dimer.[21,22]

These findings can be denoted as *bond anomalies* in the sense that the observed BLBS is not in line with the Badger rule. It is typical of these examples that bond anomalies are found when the bond in question connects electronegative atoms possessing electron lone pairs (lp). Therefore, the well-known bond weakening caused by lp–lp repulsion might be responsible for the reverse relationship.[23] In addition, there have been claims that reverse BLBS relations are found for bonds involving heavier elements, e.g., Pb-P and Pb-C bonds,[24] Cr-H bonds,[25] or Ti-P bonds.[26,27] In the latter cases, lp–lp repulsion does not play an important role so that alternative electronic effects had to be invoked to explain the reported bond anomalies.

Most of the studies mentioned above were based on vibrational spectroscopy or quantum chemical calculations. One also used bond dissociation energies (BDE) or bond dissociation enthalpies (BDH), electron density values, bond orders, and other parameters to postulate reverse BLBS relationships. Any of these studies can be questioned for principal reasons and therefore a critical analysis of reverse BLBS relationships preferably based on high-accuracy quantum chemical data is desirable. The preferred tool in this work will be a dynamical model of the bond strength based on vibrational spectroscopy and the theory of local modes, which was introduced by Konkoli and Cremer[28] and which, since then, has been proved to be physically sound, generally applicable, and a direct way of determining the intrinsic strength of a bond.[29–31] The usefulness of the local vibrational mode description of the bond strength has been documented by the characterization of CC bonds,[29,32–34] NN bonds,[35] CO bonds,[36] CX bonds with X = F, Cl, Br, I,[37–40] H-bonding,[41–44] pnicogen bonding,[45,46] and the characterization of isotopomers.[47]

The main objectives of this work are (i) to critically re-evaluate previously published reverse BLBS relationships, (ii) to introduce reliable bond strength orders (BSOs) needed for characterizing unusual bonds, (iii) to elucidate the interplay of electronic and electrostatic factors determining the stability of electron-rich bonds, and (iv) to derive a rational for any deviation from the commonly known inverse BLBS relationships.

E. Kraka, D. Setiawan, D. Cremer
Department of Chemistry, Computational and Theoretical Chemistry Group (CATCO), Southern Methodist University, 3215 Daniel Ave., Dallas, Texas 75275-0314
E-mail: ekraka@smu.edu

The interplay between bond length and bond strength is complex and an investigation that clarifies why deviations from the expected inverse BLBS relations occur, is timely and will lead to a deeper understanding of chemical bonding. In particular in crystal engineering, for the design of new materials, and the production of fine chemicals knowledge about how to accurately predict the strength of a chemical bond is of paramount importance.[48,49] To the best of our knowledge, no attempts have been made so far to apply vibrational spectroscopy to a systematic study of bond anomalies.

To fulfill the objectives of this work, a larger number of quantum chemical calculations has been carried out the results of which are presented in the following form. In Computational Methods section, the computational methods used in this work are described. Results are presented in Results and Discussion section together with a discussion of those bond anomalies that have become known or were investigated for the first time in this work. Finally, the conclusions of this work are summarized.

Computational Methods

Equilibrium geometries and normal vibrational modes of molecules **1**-**42** were calculated using coupled cluster theory with single (S) and double (D) excitations and a perturbative treatment of triple (T) excitations (CCSD(T))[50] employing Dunning's aug-cc-pVTZ basis sets.[51–53] Preliminary calculations were carried out at the DFT (density functional theory) level of theory employing the B3LYP hybrid functional[54–57] with the same basis set. All DFT calculations were carried out using an ultrafine grid[58,59] and tight convergence criteria in the geometry optimizations (forces and displacements $\leq 10^{-6}$ a.u.; changes in the density matrix: $\leq 10^{-8}$) to guarantee a reliable calculation of vibrational properties.

The $N_{vib} = 3N - L$ (N: number of atoms; L: number of translations and rotations of the molecule) normal vibrational modes of a molecule, their vibrational frequencies, and force constants were calculated by solving the Wilson equation.[60] The corresponding N_{vib} local vibrational modes, their frequencies ω_n^a, and force constants k_n^a were determined according to the following procedure.[28–31,61] Normal vibrational modes are coupled via electronic and kinematic coupling.[28,60] By solving the Wilson equation, electronic coupling can be eliminated whereas kinematic coupling remains. Konkoli and Cremer showed that a local-equivalent of the Wilson equation based on mass-decoupled Euler-Lagrange equations leads to local, completely decoupled vibrational modes, which relate to the normal vibrational modes via an adiabatic connection scheme.[30,31,61] A local vibrational mode vector $\mathbf{a}_n$ can be expressed in terms of normal vibrational mode vectors $\mathbf{d}_\mu$ given in terms of internal coordinates q_n according to Ref. [30]

$$\mathbf{a}_n = \frac{\mathbf{K}^{-1}\mathbf{d}_n^\dagger}{\mathbf{d}_n\mathbf{K}^{-1}\mathbf{d}_n^\dagger} \tag{1}$$

where the matrix $\mathbf{K}$ is the diagonal force constant matrix, $\mathbf{d}_n$ denotes a row vector of the matrix $\mathbf{D}$, which contains in its

columns vectors $\mathbf{d}_\mu$. The local mode force constant k_n^a of mode n (superscript a denotes that the local modes are adiabatically relaxed) is determined by eq. (2):

$$k_n^a = \mathbf{a}_n^\dagger \mathbf{K}\mathbf{a}_n = \left(\mathbf{d}_n\mathbf{K}^{-1}\mathbf{d}_n^\dagger\right)^{-1} \tag{2}$$

and the corresponding local mode frequency ω_n^a is given by Ref. [28]

$$4\pi^2 c^2 (\omega_n^a)^2 = k_n^a G_{nn} \tag{3}$$

with G_{nn} being a diagonal element of the Wilson G-matrix and defining the reduced mass of the local mode $\mathbf{a}_n$.[28]

Many of the molecules considered in this work adopt a pyramidal structure where the degree of pyramidalization plays an important role in the discussion. The latter was measured by determining for an $AH_n X_m$ molecule that normal vector, which forms with the three AH or AX bond vectors one and the same angle α. The pyramidalization angle was defined as $\theta = \alpha - 90°$ so that the planar form of $AH_n X_m$ is identified by $\theta = 0°$.

BDE and BDH (298) values were calculated with the G4 method.[62] All BDEs reported in this work do not include zero-point energies because only the electronic factors influencing their magnitude will be considered. NBO (natural bond order) charges[63–65] were determined at the CCSD(T)/aug-cc-pVTZ and B3LYP/aug-cc-pVTZ level of theory. The intrinsic strength of a bond AB is given by the local stretching force constant $k^a(AB)$,[35] which was obtained at the CCSD(T) level of theory for all bonds of the molecules investigated.

When comparing a large set of $k^a(AB)$ values the use of a relative bond strength order (BSO) n is convenient. The relative BSO $n(AB)$ is obtained by utilizing the extended Badger rule,[3,35] according to which n is related to the local stretching force constant k^a by a power relationship. The latter is fully determined by two reference values and the requirement that for a zero force constant n becomes zero. For example, the $n = f(k^a)$ relationship can be set up for NO bonds by using as the appropriate reference molecules hydroxylamine (**31**; $n(NO) = 1.0$) and nitroxyl (**34**; $n(NO) = 2.0$). In this way, the following equation is obtained:[3,35,41]

$$n(NO) = a(k)^b \tag{4}$$

with constants $a = 0.402$ and $b = 0.669$ (CCSD(T)/aug-cc-pVTZ; B3LYP: $a = 0.432$; $b = 0.617$).

Since most of the bonds investigated in this work are known as single bonds A—X, the definition of a A═X double bond was not possible or at least problematic. In this situation, it helps that there should be only a single $n = f(k^a)$ relationship, which directly describes the intrinsic bond strength AB irrespective of which period A or B belongs to. Therefore, suitable BSO values $n(AX)$ were calculated by scaling this relationship with the $k^a(NF)$ value of H_2NF (**5**) for NF bonds, H_2NCl (**10**) for NCl bonds, H_2PF (**14**) for PF bonds, and H_2AsF (**18**) for As-F bonds. For these reference molecules, BSO $n(AX)$

Journal of COMPUTATIONAL CHEMISTRY

#	Molecule (State), Sym.	B3LYP/aug-cc-pVTZ				CCSD(T)/aug-cc-pVTZ				G4	
		R(AX)	ω^a(AX)	k^a(AX)	n(AX)	R(AX)	ω^a(AX)	k^a(AX)	n(AX)	BDE(AX)	BDH(AX)
	N-F, O-F bonds										
2	HN-F$^\bullet$ ($^2A''$), C$_s$	1.374	1034	5.079	1.128	1.371	1035	5.088	1.148	74.17	71.71
3	FN-F$^\bullet$ ($^2B_1$), C$_{2v}$	1.356	971	4.480	1.044	1.347	1005	4.802	1.104	67.75	66.70
5	H$_2$N-F($^1A'$), C$_s$	1.433	938	4.176	1.000	1.427	934	4.142	1.000	73.10	69.27
6	H(F)N-F($^1A'$), C$_s$	1.402	911	3.938	0.964	1.394	923	4.047	0.985	68.30	65.69
7	F$_2$N-F($^1A_1$), C$_{3v}$	1.379	875	3.637	0.918	1.369	920	4.021	0.981	59.75	58.27
8	HN-Cl$^\bullet$ ($^2A''$), C$_s$	1.694	751	3.326	1.124	1.689	762	3.423	1.112	63.50	61.59
9	ClN-Cl$^\bullet$ ($^2B_1$), C$_{2v}$	1.715	660	2.565	0.958	1.707	688	2.787	0.969	46.66	46.28
10	H$_2$N-Cl($^1A'$), C$_s$	1.768	683	2.750	1.000	1.758	704	2.920	1.000	63.59	60.44
11	H(Cl)N-Cl($^1A'$), C$_s$	1.771	626	2.312	0.898	1.759	665	2.607	0.927	49.69	47.97
12	Cl$_2$N-Cl($^1A_1$), C$_{3v}$	1.782	567	1.894	0.794	1.767	621	2.271	0.845	37.08	36.44
14	H$_2$P-F($^1A'$), C$_s$	1.629	786	4.284	1.000	1.617	814	4.601	1.000	113.69	111.29
15	H(F)P-F($^1A'$), C$_s$	1.608	811	4.565	1.040	1.594	848	4.985	1.055	124.12	122.20
16	F$_2$P-F($^1A_1$), C$_{3v}$	1.591	828	4.758	1.066	1.575	873	5.283	1.097	133.66	132.31
18	H$_2$As-F($^1A'$), C$_s$	1.772	646	3.721	1.000	1.744	692	4.276	1.000	102.41	100.54
19	H(F)As-F($^1A'$), C$_s$	1.750	657	3.851	1.022	1.721	721	4.640	1.056	110.46	109.01
20	F$_2$As-F($^1A_1$), C$_{3v}$	1.732	684	4.177	1.074	1.701	746	4.975	1.106	118.27	117.24
21	H$_2$C=N-F($^1A'$), C$_s$	1.419	884	3.713	0.930	1.412	888	3.747	0.935	68.82	66.10
22	:C=N-F($^1\Sigma^+$), C$_{\infty v}$	1.307	1205	6.900	1.363	1.306	1200	6.839	1.399	54.47	53.02
23	:N-F($^3\Sigma^-$), C$_{\infty v}$	1.320	1144	6.217	1.278	1.318	1144	6.217	1.312	77.65	76.83
24	HN=N-F,cis($^1A'$), C$_s$	1.511	611	1.773	0.589	1.486	640	1.943	0.603	61.17	58.37
25	HN=N-F,tr($^1A'$), C$_s$	1.438	752	2.686	0.762	1.418	810	3.118	0.827	59.55	56.50
26	FN=N-F,cis(^1A_g), C$_{2h}$	1.391	874	3.626	0.916	1.382	902	3.868	0.955	21.90	20.12
27	FN=N-F,tr(^1A_g), C$_{2h}$	1.387	942	4.217	1.006	1.380	976	4.522	1.061	20.62	18.92
29	HO-F($^1A_1$), C$_s$	1.431	985	4.963	1.000	1.437	920	4.326	1.000	50.22	47.91
30	FO-F($^1A_1$), C$_{2v}$	1.403	931	4.435	0.933	1.407	888	4.032	0.954	39.94	39.12
	N-H, P-H, As-H, O-H										
1	HN-H$^\bullet$ ($^2B_1$), C$_{2v}$	1.027	3378	6.320	0.978	1.023	3419	6.474	0.982	139.40	133.48
4	H$_2$N-H($^1A_1$), C$_{3v}$	1.013	3503	6.796	1.000	1.012	3528	6.894	1.000	114.77	106.73
13	H$_2$P-H($^1A_1$), C$_{3v}$	1.421	2383	3.267	0.799	1.414	2422	3.373	0.814	87.15	82.08
17	H$_2$As-H($^1A_1$), C$_{3v}$	1.525	2184	2.794	0.762	1.501	2282	3.051	0.791	78.84	74.34
28	HO-H($^1A_1$), C$_{2v}$	0.962	3829	8.191	1.059	0.959	3870	8.367	1.057	124.95	118.13
	References:										
	NO, NS, and NSe bonds										
31	H$_2$N-OH($^1A'$), C$_s$	1.445	942	3.902	0.959	1.443	942	3.905	0.962	69.08	62.98
32	H$_2$N-SH($^1A'$), C$_s$	1.732	699	2.805	0.826	1.730	723	2.995	0.851	70.76	66.14
33	H$_2$N-SeH($^1A'$), C$_s$	1.878	593	2.471	0.811	1.854	628	2.768	0.864	63.10	58.98
34	HN=O($^1A'$), C$_s$	1.198	1652	12.005	1.918	1.210	1582	11.007	1.923	167.50	164.71
35	HN=S($^1A'$), C$_s$	1.571	1077	6.649	1.406	1.584	1025	6.033	1.359	124.67	122.47
36	HN=Se($^1A'$), C$_s$	1.720	879	5.427	1.318	1.725	843	4.986	1.281	106.22	104.31
	PO and AsO bonds										
37	H$_2$P-OH($^1A'$), C$_s$	1.677	782	3.796	0.912	1.669	808	4.055	0.943	93.22	88.91
38	H$_2$As-OH($^1A'$), C$_s$	1.821	644	3.226	0.814	1.792	692	3.718	0.881	81.24	77.59
39	HP=O($^1A'$), C$_s$	1.492	1208	9.076	1.561	1.497	1179	8.633	1.563	184.64	182.98
40	HAs=O($^1A'$), C$_s$	1.634	966	7.244	1.341	1.636	951	7.031	1.350	157.57	156.38
	FH bonds										
41	F$\cdots$H$\cdots$F$^-$ ($^1\Sigma_g^+$), D$_{\infty h}$	1.149	1361	1.044	0.551	1.138	1241	0.868	0.550	43.23	43.96
42	F-H($^1\Sigma^+$), C$_{\infty v}$	0.922	4090	9.432	1.102	0.919	4139	9.660	1.101	141.31	136.40

[a] Distance R(AX) in Å, local stretching frequencies ω^a(AX) in cm^{-1}, local AX stretching force constants k^a(AX) in mdyn Å^{-1}, and bond strength order n(AX). For molecular structures and NBO charges, see Figure 1.

becomes 1.0 and makes a meaningful comparison of a group of AX bonds possible. This approach was tested by calculating the relative BSO values of reference molecules **32**, **33** (N-S and N-Se single bond), and **34** to **40** (formal double bonds N=S, N=Se; single bonds P-O, As-O, formal double bonds P=O, As=O). In all cases, reasonable BSO values were obtained, which qualitatively changed parallel to the calculated BDE values for these bonds (Table 1). In a similar way, the BSO values of A-H bonds were determined using the FH

bonds in $F\cdots H\cdots F^-$ (**41**; n(FH) = 0.5) and FH (**42**; n = 1.0) as suitable reference (CCSD(T): $a = 0.521$; $b = 0.288$; B3LYP: $a = 0.505$; $b = 0.306$) and, then scaling the resulting $n=f(k^a)$ relationship with the help of suitable reference molecules AH$_3$ (A = N, P, As).

The local vibrational modes[28] were calculated and analyzed with the program package COLOGNE2015.[66] For the CCSD(T) calculations, the program CFOUR[67,68] was used whereas for the DFT calculations Gaussian09[69] was employed.
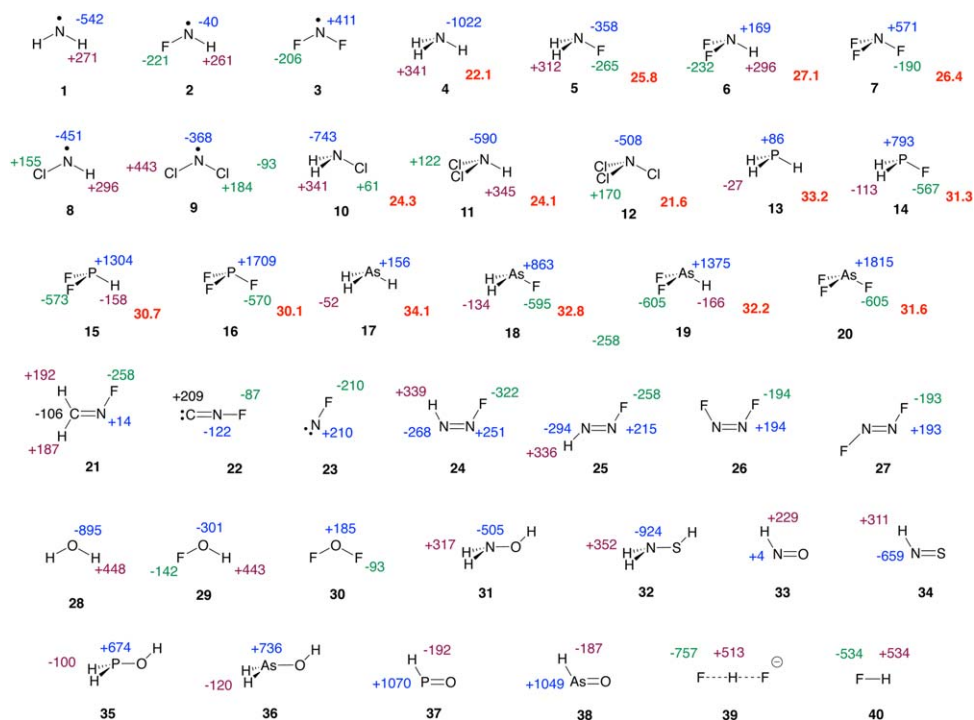
Figure 1. Structures **1** to **40** with CCSD(T)/aug-cc-pVTZ atomic charges (NBO) given in melectron: Blue: central atom; green: halogen atom; brown: H atom; black: other atoms. The bold red number give the pyramidalization angle θ. [Color figure can be viewed in the online issue, which is available at wileyonlinelibrary.com.]

Results and Discussion

In Table 1, AX bond properties of compounds **1** to **42** (compare with Fig. 1) calculated at the B3LYP/aug-cc-pVTZ and CCSD(T)/aug-cc-pVTZ levels of theory are listed. These comprise the distance $R(AX)$ for A = N, P, As, O and X = F, Cl, and H, the corresponding local stretching frequency $\omega^a(AX)$, the local stretching force constant $k^a(AX)$, the relative BSO value $n(AX)$ as well as the corresponding G4 BDE(AX), and BDH(AX) values. Table 2 gives a short summary of the results of the NBO delocalization values. Geometries of the molecules investigated (Cartesian coordinates and trends in the bond lengths and bond angles can be found in the Supporting Information). In Figure 1, the CCSD(T) NBO charges and the pyramidalization angles θ are summarized. In Figure 2 the CCSD(T) geometries for **1**–**20** are shown; (a) equilibrium geometries, (b) planar geometries. Figure 3 gives the relative BSO(NF) values for all NF bonds investigated in this work, which stretch from 0.8 to 1.4.

Reverse BLBS relationships in fluoro amines

Various investigations have discussed a reverse BLBS relationship for the NF bonds of the fluoro amines.[9–12] At first sight (see Fig. 4a and Table 1), the CCSD(T) results obtained in this work suggest a normal, Badger-type BLBS behavior for all NF bonds of molecules **2** to **27**. A Badger-type behavior is also found for the NH bonds listed in Table 1.

A closer inspection of the scattering in the N-F bonds with regard to a general BLBS relationship reveals that for the fluoro amine radicals HNF (**2**) and FNF (**3**, green line in Figs. 4a and 4b) as well as the fluoro amines NH$_2$F (**5**), NHF$_2$ (**6**), and NF$_3$ (**7**, blue line in Figs. 4a and 4b), the NF bond strength presented by the local NF stretching force constant increases with increasing NF bond length (see also Table 1) suggesting a reverse BLBS relationship. The effects are relatively small compared to the total variation in the NF bond length from 1.30 to almost 1.43 Å (Fig. 4a), but they are confirmed by the B3LYP results and the G4 BDE values, which change from 73.1 to 68.3 and 59.7 kcal/mol with increasing fluorination and decreasing NF bond length (Table 1). All values indicate an inverse BLBS relationship and by this a *bond anomaly* where we associate this term with the observation that the shorter bond corresponds to the weaker rather than stronger bond. To find a rational for the N-F bond anomaly, we will develop a suitable electronic structure model and test its usefulness by systematically varying the target molecules and scrutinizing whether the model chosen can rationalize the changes in bond strength observed without any inherent contradictions.

The length of a bond can be estimated by using standard covalent radii for the atoms involved. Those found in the literature for N and F (0.71 and 0.57 Å (Cambridge covalent radii)[70] were derived for A-H bonds in hydrides and therefore they are too small. Utilizing H$_2$NF as a suitable reference molecule (CCSD(T) NF bond length: 1.427 Å; Table 1) and keeping the ratio of the Cambridge covalent radii, one obtains improved radii of 0.792 (N) and 0.635 Å (F), respectively. Other covalent radii have been suggested by Politzer and Murray[71,72] but the values given above are *ad hoc* radii to reproduce the CCSD(T) value of the NF bond length in **5**, which is the reference bond for discussing the NF bonds of the

Table 2. Results of the NBO analysis (in form of delocalization energies and changes in lone pair orbital energies) and bond length analysis.[a]

#	Mol	ΔE (Mult.)	#	Mol	ΔE	#	Mol	ΔE	#	Mol	ΔE
Anomeric delocalization energies lp(X) → σ*(AX) for pyramidal forms											
3	NF_2	6.05 (2)	**9**	NCl_2	4.42						
5	NH_2F	1.98[b] (2)	**10**	NH_2Cl	1.73	**14**	PH_2F	3.31	**18**	AsH_2F	< 0.50
6	NHF_2	11.90 (2)	**11**	$NHCl_2$	7.34	**15**	PHF_2	10.10	**19**	$AsHF_2$	8.84
7	NF_3	7.15 (6)	**12**	NCl_3	3.62	**16**	PF_3	5.50	**20**	AsF_3	4.60
		4.45 (6)			3.30			4.40			3.83
Anomeric delocalization energies lp(X) → σ*(AX) for planar forms											
5	NH_2F	7.23[b] (2)	**10**	NH_2Cl	4.60	**14**	PH_2F	6.98	**18**	AsH_2F	5.34
6	NHF_2	15.33 (2)	**11**	$NHCl_2$	8.58	**15**	PHF_2	11.07	**19**	$AsHF_2$	8.95
7	NF_3	12.25 (6)	**12**	NCl_3	6.06	**16**	PF_3	4.99c)	**20**	AsF_3	4.07c)
					2.49						
Increase in the A(lp) energy upon planarization											
4	NH_3	0.0983				**13**	PH_3	0.2371	**17**	AsH_3	0.3151
5	NH_2F	0.1745	**10**	NH_2Cl	0.1570	**14**	PH_2F	0.2497	**18**	AsH_2F	0.3238
6	NHF_2	0.2342	**11**	$NHCl_2$	0.2088	**15**	PHF_2	0.2617	**19**	$AsHF_2$	0.3308
7	NF_3	0.2795	**12**	NCl_3	0.2566	**16**	PF_3	–[c]	**20**	AsF_3	–[c]
#	Mol	ΔR (ΔR_{pl})	#	Mol	ΔR (ΔR_{pl})	#	Mol	ΔR (ΔR_{pl})	#	Mol	ΔR (ΔR_{pl})
Changes in NF bond length relative to AH_2X: pyramidal (upon planarization)											
5	NH_2F	0[d] (−42)	**10**	NH_2Cl	0[d] (−66)	**14**	PH_2F	0[d] (−18)	**18**	AsH_2F	0[d] (−17)
6	NHF_2	−33 (−42)	**11**	$NHCl_2$	1 (−75)	**15**	PHF_2	−23 (−10)	**19**	$AsHF_2$	−23 (−9)
7	NF_3	−58 (−27)	**12**	NCl_3	9 (−80)	**16**	PF_3	−42 (–)[c]	**20**	AsF_3	−43 (–)[c]

[a] Block 1 and 2: Delocalization energies ΔE in kcal/mol for the anomeric delocalization of the halogen electron lone pairs into vicinal σ*(NX) orbitals. Only in the case of the H_2A-X molecules, the delocalization into a σ*(NH) orbital (indicated by the abbreviation NH) is given for reasons of comparison. Numbers in parentheses placed in the third column, define the multiplicity (Mult.) of a ΔE value, i.e. how often a given ΔE value occurs because of symmetry and the number of halogen atoms. Block 3: Increase of the lp(A) orbital energy relative to the corresponding orbital energy of the pyramidal form given in Hartrees. For **16** and **20**, D_{3h}-symmetrical PF_3 and AsF_3 represent Jahn-Teller unstable systems. Therefore, they are excluded for the comparison. Block 4: Bond lengths changes ΔR in $10^3 \times$Å relative to the R value of ANH_2X upon increasing halogenation are given where a positive (negative) sign indicates an increase (decrease) of R relative to the reference bond length or, given in parentheses, the change in the bond length of the planar form relative to that of the pyramidal form. CCSD(T)/aug-cc-pVTZ calculations (geometry), B3LYP/aug-cc-pVTZ calculations in the case of the NBO delocalization energies and the lone pair energies. [b] Delocalization into a σ*(NH) orbital. [c] The D_{3h} form is Jahn-Teller unstable and corresponds to a second-order TS. [d] Reference bond lengths are 1.427 (**5**), 1.758 (**10**), 1.617 (**14**), and 1.744 Å (**18**).

fluoroamines. It is well-known that the covalent radius of an atom decreases with increasing electron withdrawal or, in general, increasing oxidation state as has been shown for transition metal cations.[73,74] The strong withdrawal of negative charge from N caused by several F atoms leads to change in the N atomic population from −1022 melectron (me) in NH_3 to +571 me in NF_3, i.e. to a change by 1593 me according to CCSD(T)-NBO calculations (Fig. 1). The N atom converts from an atom with an anionic to one with a cationic charge distribution and accordingly its covalent radius decreases from H_2NF to NF_3 by about 0.05 Å, which is a large change for an electronegative element with a tight electron density distribution.

The drastic decrease of the NF bond length with increasing fluorination can lead to different electron structure changes: (i) the exchange repulsion between the lone-pair electrons of N and F (through-bond or through-space lp-lp repulsion) should significantly increase and destabilize the NF bond. Destabilization by lp-lp repulsion is reduced by charge withdrawal from N, anomeric delocalization, or geometry relaxation. Therefore, the magnitude of this effect can be only estimated indirectly, e.g. by considering the increase of the N lone pair orbital energy upon planarization of a pyramidal molecule (Table 2 and below). Increasing pyramidalization from $\theta = 22.1°$ in NH_3 to $\theta = 26.4°$ in NF_3 can lower through bond lp-lp repulsion to

some degree; however, only at the price of increasing through-space lp(F)-lp(F) repulsion. (ii) Anomeric delocalization of a halogen electron lone pair into a vicinal low-lying σ*(NX) orbital leads to NX bond weakening where however, it has to be considered that lone pair delocalization adds some π-character to the YN bond if Y is the donor. Since bond strengthening via increased π-character is less efficient than σ-bond weakening the overall effect in NHX_2 or NX_3 leads to NX bond weakening, which can be quantitatively assessed by the NBO analysis via its delocalization energies. (iii) Also, hyperconjugation effects, e.g. by charge delocalization from a σ(NH) orbital to a σ*(NX) orbital can play a role. However, the NBO analysis reveals that these effects are relatively small compared to anomeric delocalization and should not affect the NX bond length significantly. There is also the possibility that effect (i), (ii), and (iii) act at the same time. In this connection, the data in Table 2 provides some guidance although the discussion of lp-lp repulsion in connection with bond weakening is still problematic.

Before continuing the discussion, we would like to point out that the NBO analysis for effect ii) is based on localized molecular orbitals (LMOs) whereas sometimes a more elegant representation of an electronic effect may be based on the electronic wavefunction generated from canonical MOs. For example, many electronic features have been explained in
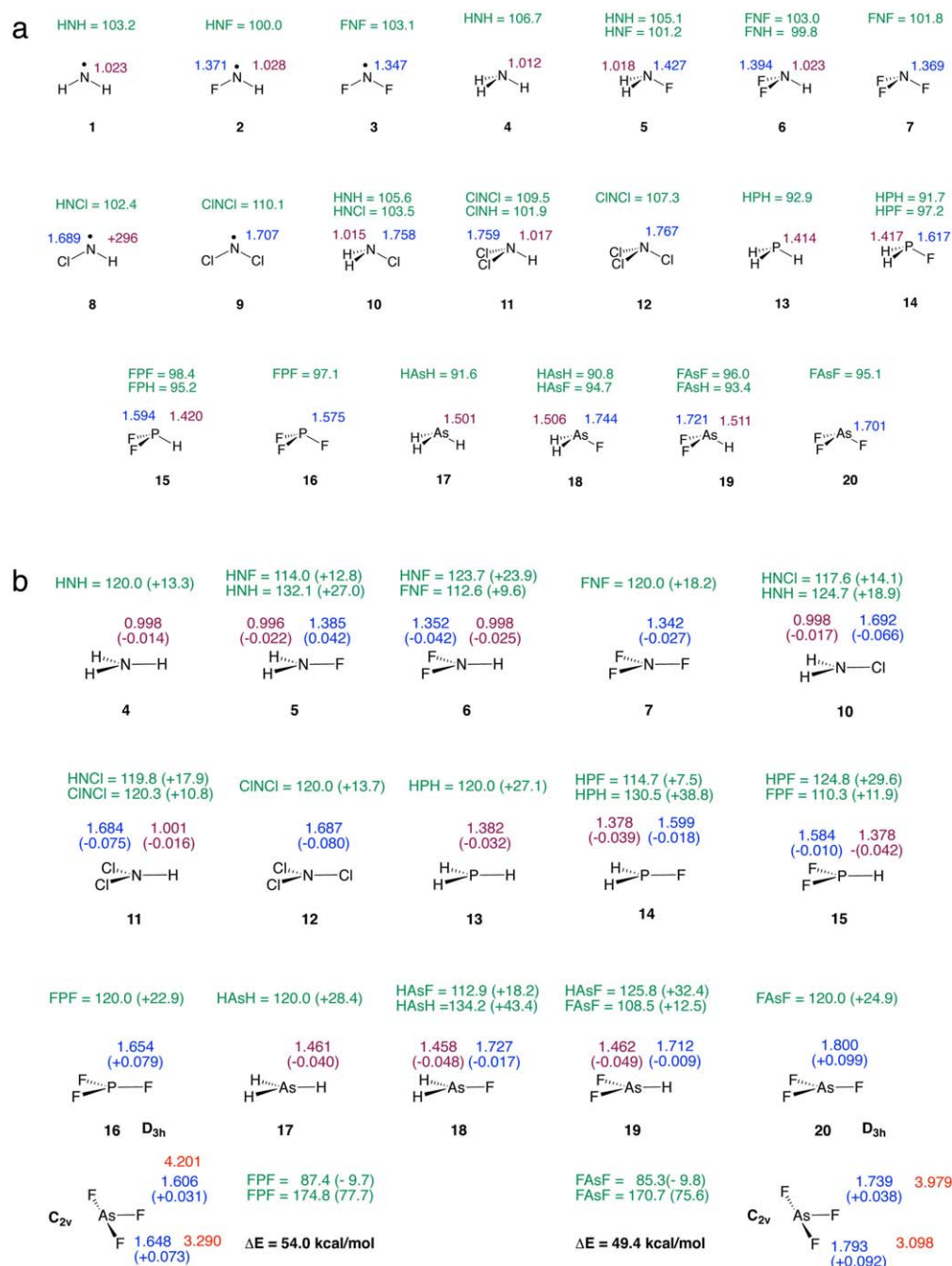
Figure 2. CCSD(T)/aug-cc-pVTZ geometries and changes of molecules **1** to **20**. a) Equilibrium geometries. b) Planar geometries. For planar **16** and **20**, the second-order TS of D_{3h}-symmetry, which are Jahn-Teller unstable) and the first order saddle points of C_{2v}-symmetry are both reported together with the barriers of planarization. Bond lengths in Å, bond angles in degrees, and barriers to planarity in kcal/mol. Numbers in parentheses give the changes in the geometry upon planarization.

terms of pseudo-Jahn-Teller effects invoking interactions between ground state and excited states according to well-specified symmetry rules.[75] In a simplified way, pseudo-Jahn-Teller effects can be expressed as second-order Jahn-Teller (SOJT) effects using canonical MOs rather than state wave functions. An explanation of bond weakening in the course of a SOJT effect implies that one considers changes in hybridization. This leads to the well-known hybridization defect that is typical of the electronic behavior of the elements in the higher periods.[76–81] Hybridization is indirectly a result of the lack of a nodal sphere (present in the 2s atomic orbital (AO)) in the case of the 2p AOs, which makes their radial expansion comparable to that of the 2s AO and in this way facilitates sp-hybridization and the maximization of orbital overlap with partner atoms. Hence, bonding between second period atoms utilizing sp^n hybrid orbitals rather than just 2p AOs is strong provided other electronic effects do not diminish it. If a large charge at the N atom leads to a contraction of the valence
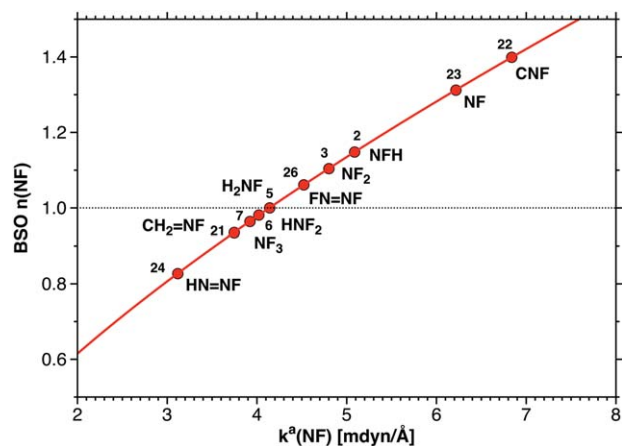
Figure 3. Relative BSO values $n(NF)$ given as a function of the corresponding local stretching force constants k^a according to CCSD(T)/aug-cc-pVTZ calculations. [Color figure can be viewed in the online issue, which is available at wileyonlinelibrary.com.]

orbitals, the 2s AO with its nodal sphere will be more effected than the 2p AOs with their angular nodal planes that contain the position of the corresponding nucleus. Hence, the radial expansion of the 2s AO will become significantly smaller than that of the 2p AOs, hybridization does deteriorate (hybridization defect), and the NF bonds become weaker.

Either explanation (i), (ii), or a superposition of these electronic effects can explain the reverse BLBS relationships for the fluoro amines (see Fig. 5). We will in the following systematically analyze which of these electronic effects is dominant and for this purpose we will vary the structure of the fluoro amines in the following way: (1) by increasing the lp effect, e.g. in planar $H_n NF_{3-n}$, its relevance can be tested. (2) By replacing F with Cl the electronegativity of the substituent is decreased and by this also the positive charge at N. In this way, we will see how important charge contraction is. (3) Third or fourth period atoms A such as P or As, should be a better charge donor to F and the bond length contractions should be substantial. However, P or As could also lead to a variation of (i) or (ii) in Figure 5. (4) A central atom such as O will have the opposite effect on any charge contraction as P or As. Again, the consequences (i) and (ii) can be tested. (5) Finally, it is interesting to replace in a fluoro amine two H atoms by a substituent that may have an effect on the NF bond length and bond strength such as in molecules **21** to **27**.

Planarization of the Fluoro Amines. If through-bond lp(A)-lp(X) repulsion would be exclusively responsible for the weakening effect causing NF bond anomalies, the latter should be increased for planar AX$_3$ molecules. In Figure 6, the NF bond properties of the planar systems calculated in this work are summarized. All structures are first order saddle points (transition states of the inversion at the central atom A) with the exception of **16** and **20** where three imaginary frequencies indicate an in-plane (ip) SOJT distortion from $D_{3h}-$ to $C_{2v}-$symmetry.[82] The latter forms have different AF bonds (P: 1.606; 1.648; As: 1.739, 1.793 Å) and force constants (P: 3.819, 2.921; As: 3.529; 2.732 mdyn/Å; planarization barriers ΔE: 54.0

(P) and 49.4 kcal/mol (As)) and therefore are not included into the comparison.

Comparison of the NF bond lengths and local stretching force constants reveals an overall bond shortening relative to the pyramidal forms (see Table 2) because of a change from sp^3 to sp^2 hybridization and improved overlap. Again, the N charges reveal that charge withdrawal from N and the concomitant contraction of covalent radius is responsible for bond shortening with increasing fluorination. Unexpected is the fact that the NF bond is strengthened with increasing fluorination despite the increase in lp(N,2pπ)-lp(F,2pπ) repulsion at a shorter NF bond length as is reflected by the energy raising of the N lone pair orbital upon planarization (Table 2). This is in contradiction with the assumption that the NF bond anomalies of the pyramidal forms are a result of through-bond lp-lp repulsion.

In view of the results for the planar fluoro amines, the assumption that through-bond lp-lp repulsion is the major cause for the observed bond anomalies has to be discarded. In this connection, it is important to emphasize that the pyramidalization of NH$_3$ is a direct consequence of the SOJT effect[83–86] involving the two a_1-symmetrical frontier orbitals. The closer these two orbitals are in the planar form, the
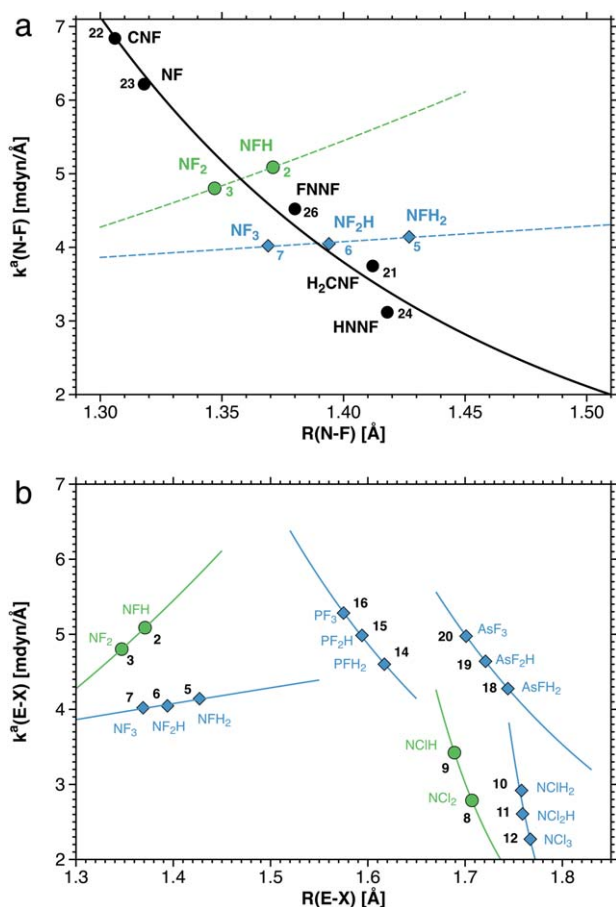

Figure 4. Inverse and reverse BLBS relationships for a) NF bonds and b) NF bonds in comparison with NCl, PF, and AsF bonds. CCSD(T)/aug-cc-pVTZ calculations. [Color figure can be viewed in the online issue, which is available at wileyonlinelibrary.com.]
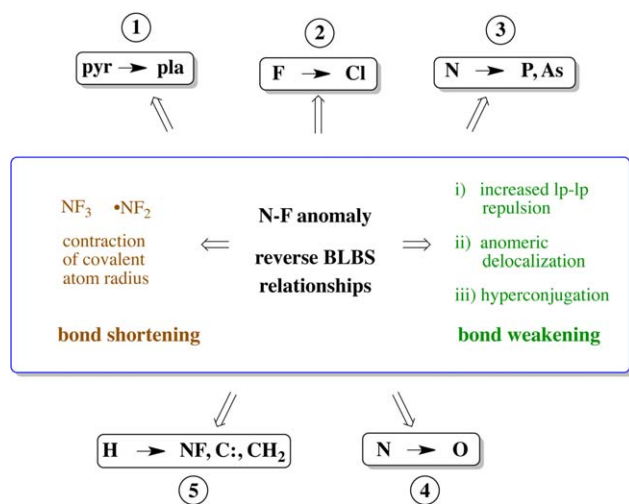
Figure 5. Strategic scheme for the investigation of the NF bond anomaly in fluoro amines by stepwise changing the structure (pyr: pyramidal *vs.* pla: planar), replacing the central atom, or the substituents by other atoms or groups (steps 1–5). The major reasons for the bond anomaly (left: bond contraction; right: bond destabilization) are given. [Color figure can be viewed in the online issue, which is available at wileyonlinelibrary.com.]

stronger is the molecule pyramidalized, the stronger is the mixing of the frontier orbitals upon pyramidalization, and the stronger is the overall stabilization of the molecule.

The change from a more electronegative central atom A to a more electropositive A leads to an increase of the HOMO energy (the $p\pi(A)$ orbital) whereas the LUMO, which is substituent-dominated, changes only little in energy. Accordingly, the HOMO-LUMO energy gap becomes smaller, frontier orbital mixing stronger, the pyramidalization angle θ and the barrier to planarity larger, and AX bonding weaker in view of an increased *p*-character of the AX bonding orbitals. Conversely, replacing the substituents by more electronegative atoms or functional groups lowers the LUMO in energy, again the HOMO-LUMO gap is decreased, and pyramidalization is increased. These are well-known facts[86] and explain the trends in the calculated barriers (ΔE: 5.5 (**4**) to 83.4 kcal/mol (**7**, Fig. 6) and pyramidalization angles θ of the fluoro amines (22.1 (**4**) to 26.4 (**7**), Fig. 1).

Clearly, through bond $lp(\pi)$-$lp(\pi)$ repulsion also destabilizes the planar form and adds to the high energies of the planar forms although it does not dominate the NF bond strength. This seems to result from the lower population of the $p\pi(N)$ orbital, which looses up to 50% of its charge with increasing fluorination. Another electronic effect influences the NF bond strength in the planar forms: For planar **6**, the FNF angle is decreased from 120 in **7** to 112.6° despite the potentially strong ip through space lp-lp repulsion between the F atoms. Clearly, this is a result of the mutual anomeric delocalization of the ip lp(F) electrons into the neighboring $\sigma^*(NF)$ orbital, which is more efficient for bond angles closer to 90° and which does not necessarily lead to bond strengthening of the NF bonds (because it takes place for a NF$_2$ group in both directions) but to a lowering of through-space lp(F)-lp(F) repulsion.

In the case of pyramidalized fluoro amines, bond weakening is caused by lp-lp repulsion and anomeric delocalization. For example, for pyramidalized **6** and **7**, an increase in through-space lp(F)-lp(F) repulsion enhances NF bond weakening. Indicative of this is the fact that the pyramidalization angle first increases ($\theta = 25.8$ to 27.1°) and then decreases again (26.4°, Fig. 1). In the planar forms, the same effects are active, however, with the result that because of better pπ-pπ overlap and a contraction of the orbitals (enhanced by the larger electronegativity of a sp^2-hybridized central atom), anomeric delocalization is stronger (Table 2) as is NF π-bonding. According to the NBO analysis, there are sizable lp(N) $\rightarrow$ Ry(F) contributions (Ry: Rydberg 3p orbital; 4.13, 5.84, 6.75 kcal/mol for **5**, **6**, and **7**, respectively) enhancing pπ(N)-pπ(F) overlap thus leading to a normal inverse BSBL relationship.

Similar electronic effects determine the bond anomaly of the fluoro amine radicals. A SOJT effect is responsible for the bending of the linear molecules, which becomes stronger for AX$_2$ systems with electronegative substituents such as F. Alternatively, one can explain the bending as a result of anomeric delocalization of the ip lp(F) electron pair into the $\sigma^*(NF)$ orbital, which is maximal at 90°, and therefore favors a small bending angle (Table 2 and Fig. 2). The FNF angle is actually with 103.1° equal to the HNH angle (Fig. 2), which is due to ip through-space lp(F)-lp(F) repulsion and a subsequent widening of the FNF angle. The NF bond in **3** is weakened relative to that of **2** by the very same effects determining the bending angle. Bond weakening in radical **3** is reflected by the lower NF stretching force constant and BDE value in contradiction of the NF bond shortening from 1.371 to 1.347 Å.

Based on these findings, the prerequisites for an AX bond anomaly seem to be (i) a large electronegativity difference between A and X causing a decrease of the covalent radius of A, (ii) anomeric delocalization of lp(X) into a geminal $\sigma^*(AX)$ orbital, and (iii) through-space (but less through-bond) lp-lp repulsion where effects (ii) and (iii) lead to a weakening of the NF bond. Since the bending or pyramidalization of the molecule can be elegantly explained by a SOJT effect, there is also the possibility of rationalizing NF weakening by the hybridization defect associated with the reduction of the bond angle. In the following we will test whether this explanation model involving up to three different electronic effects can provide a rational for all inverse or reverse BLBS relationships observed in this work.

Chloro amine radicals and chloro amines. As shown in Figures 4b and 6, the BLBS relationship for the NCl bonds in both the pyramidal and planar chloro amines provides a new insight into bond anomalies. The Allred-Rochow electronegativity of chlorine (2.83) is considerably smaller than that of fluorine (4.10) and close to that of nitrogen (3.07).[87,88] Accordingly, nitrogen withdraws electrons from chlorine so that the N charge in the chloro amines is always negative (Figs. 1 and 6). The NBO-CCSD(T) values of the N atom are -451 me (**8**), -368 me (**9**), -743 me (**19**), -590 me (**11**), and -508 me (**12**) thus being 411, 779, 385, 759, and 1059 me more negative than in the corresponding fluoro amines. In the planar forms of the chloro amines
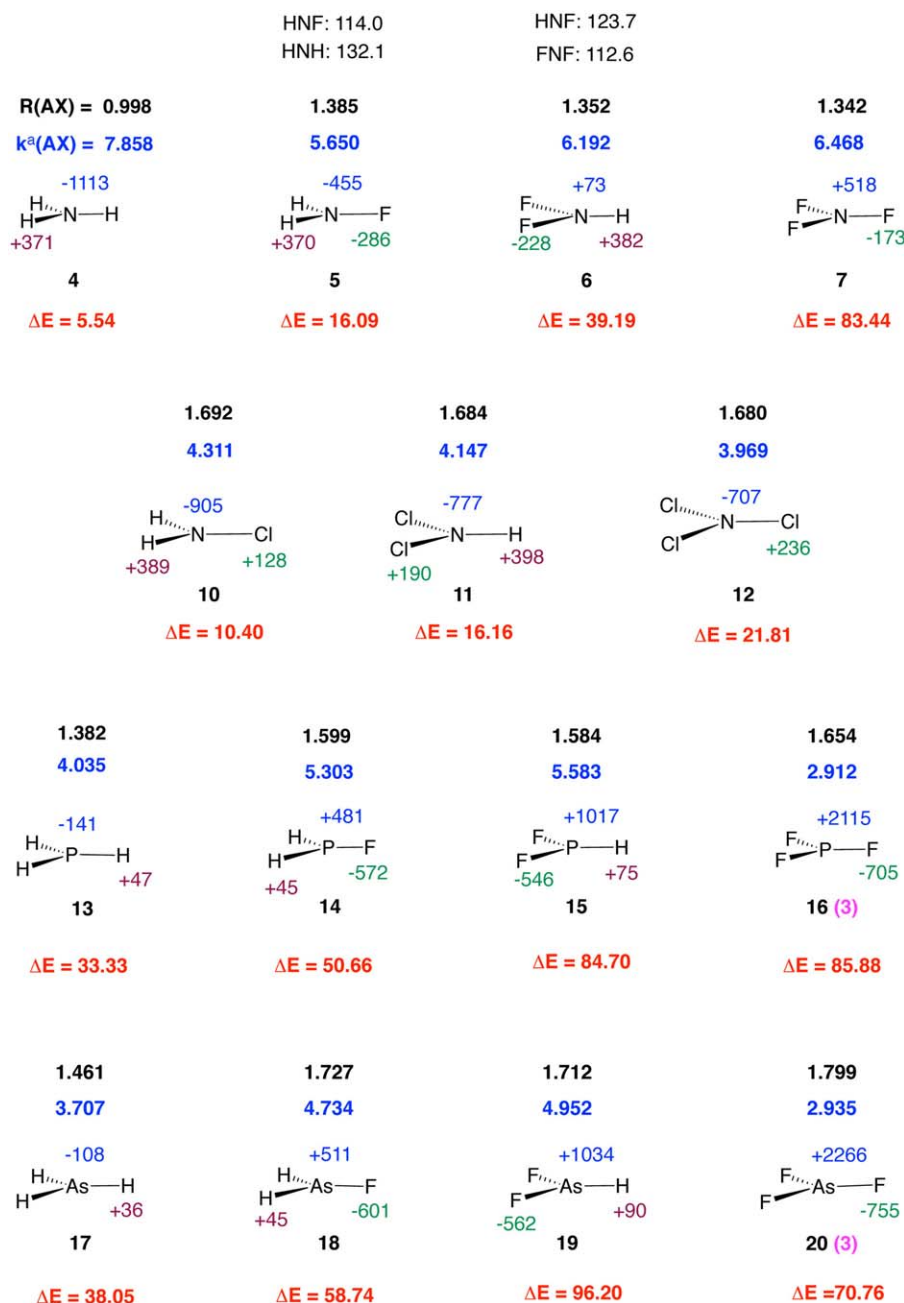
Figure 6. Planar transition states (1 imaginary frequency unless otherwise given in purple after the bold number of the molecule) of the inversion at the atom A in AX_3 according to CCSD(T)/aug-cc-pVTZ calculations. ΔE values (in red) give the barrier to planarity in kcal/mol; bold black values denote A-X distances in Å, bold blue values AX stretching force constants in mdyn/Å. In normal print, NBO charges are given for A (blue), X (green), H (brown). For **5** and **6**, bond angles (in degree) are also given. For **16** and **20**, the C_{2v}-symmetrical form with 1 imaginary frequency has an FPF (FAsF) angle of 87.4 (86.1°). [Color figure can be viewed in the online issue, which is available at wileyonlinelibrary.com.]

the negative charges are even higher, but follow the same overall trend: −905, −777, and −707 me (Fig. 6).

The accepted covalent radius of Cl (0.99 Å) is considerably larger than that of F (0.71 Å)[70] leading to longer bonds, which increase with increasing chlorination (**8**, **9**: 1.689, 1.707 Å; **10-12**: 1.758, 1.759, 1.767 Å). A normal, i.e. inverse BSBL relationship is observed, i.e. the longer NCl bonds have smaller NCl stretching force constants (Table 1). For the planar chloro amines, the bond lengths contract with increasing chlorination (1.692, 1.684, and 1.680 Å; Fig. 6) whereas their

bond strengths decreases: 4.311 (**10**), 4.147 (**11**), 3.969 mdyn/Å **12**; (Fig. 6) thus suggesting a different electronic situation than in the pyramidal chloro amines. Hence, the chloro amines follow just the opposite trends than for the fluoro amines.

For chloro amines, the SOJT effect is smaller and decreases from **10** to **12** as indicated by the lowering of the pyramidalization angles (24.3 to 21.6°) and low barriers to planarization (Figs. 1 and 6), which increase with increasing chlorination from 10.4 to 21.8 kcal/mol (Fig. 6).
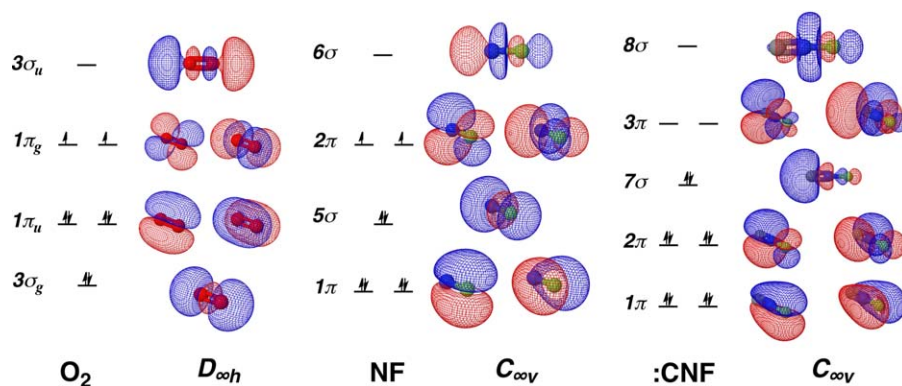
Figure 7. Valence molecular orbitals of O_2 ($^3\Sigma_g^-$),: NF ($^3\Sigma^-$, **23**), and: CNF ($^1\Sigma^+$, **22**). Restricted Hartree-Fock/6-31G(d,p) calculations.

The differing behavior of the NCl bonds (compared to that of the NF bonds) has its origin in its different bond polarity. Due to the fact that the N atom is negatively charged and Cl atoms positively, the covalent radius of N expands with increasing chlorination which is in line with the increasing anomeric delocalization and weakening of the NCl bonds. For the planar chloro amines, the shortening of the NCl bonds is due to an increased s character and the resulting increase in electronegativity of the N atom in addition to a better pπ-pπ-overlap. These trends can be easily predicted considering (i) the charge distribution, (ii) the NBO delocalization energies of Table 2 (smaller than for the NF bonds but increasing with increasing chlorination where always the multiplicity of a ΔE value, i.e. how often a given delocalization value occurs because of symmetry and the number of halogen atoms according to the number in parentheses in column 3), and (iii) the increase of the A(lp) orbital energy upon planarization. The bond anomaly of the planar chloro amines is not predictable without the NBO analysis. Contrary to the fluoro amines, the planar chloro amines possess, although anomeric delocalization is generally lower (Table 2), additional anomeric delocalization terms lp(Cl) $\rightarrow$ σ^*(NCl) (NHCl$_2$: 6.24: NCl$_3$: 14.94 kcal/mol) involving the σ-lp (strongly dominated by 3s(Cl) character), which for the planar fluoro amines does not play any role. This additional anomeric delocalization effect leads to a weakening of the NCl bonds and the observed bond anomaly.

It seems that the NX bond anomaly depends on the bond polarity of the NX bond (depending in turn on electronegativity difference between A and X), the decrease of the bond length because of a reduction of the covalent radius of A or X and/or a rehybridization from sp to sp^2 on the one side and possible bond weakening effects because of lp(A)-lp(X) repulsion (difficult to quantify) and anomeric delocalization effects. In the planar forms, anomeric delocalization involving the lp(X,π) orbitals should weaken the acceptor bond and strengthen the AX bond to the donor. However if additional anomeric delocalization involving lp(X,σ) orbitals takes place the net effect is an AX weakening. The latter effect also depends on well-tuned donor, acceptor orbital energies and bond polarity.

Fluoro phosphines and their arsenic homologues. By replacing N with P or As several electronic effects leading to a bond

anomaly should increase. The investigation of fluoro phosphines **14** to **16** and the fluoro arsines **18** to **20** reveals a drastic increase in the positive charge at the P (from +793 to +1709 me) and As atom (from +863 to +1815 me, Fig. 1), which fulfills the prerequisite for bond shortening in line with a contraction of the covalent atomic radius. The calculated R(PF) (1.617, 1.594, 1.575 Å) and R(AsF) bond lengths (1.744, 1.721, 1.701 Å) confirm this. The same holds for the planar fluoro phosphines and arsines (P: 1.599, 1.584; As: 1.727, 1.712 Å; Fig. 6) where however the second-order saddle points of **16** and **20** cannot be included into the comparison because they indicate a SOJT effect in the planar form that causes a deformation to C_{2v}-symmetrical T forms.[82] The pyramidalization angles (up to 32°; Fig. 1) and the barriers to planarity (up to 96 kcal/mol; Fig. 6) are in line with a stronger SOJT (increase of the HOMO energy; decrease of the HOMO-LUMO gap). Hence, the prerequisites for a reverse BLBS relationship and AX bond anomalies seem to be fulfilled.

However, the BSO values (based on the local PF and AsF stretching force constants increase rather than decrease: n(PF): 1.000, 1.055, 1.097 according to k^a(PF) values of 4.601, 4.985, and 5.283 mdyn/Å; n(AsF): 1.000, 1.056, 1.106 according to k^a(AsF) values of 4.276, 4.640, and 4.975 mdyn/Å (Table 1). The AsF bonds are somewhat weaker than the PF bonds in line with the calculated BDE values (P: 113.7, 124.1, 133.7; As: 102.4, 110.5, 118.3 kcal/mol; Table 1) but both PF and AsF bonds are stronger than the corresponding NF bonds according to stretching force constants and BDE values, which reflect their increased ionic character.

The observations made for the phosphines and arsines in this work help to identify the decisive electronic effects causing bond anomalies. The anomeric delocalization effects are significantly smaller for the fluoro phosphines and arsines than for the amines (Table 2) where their multiplicity has to be taken into account in each case. Additional F(lp) $\rightarrow$ Ry(P) or Ry(As) delocalization terms partially balance bond weakening caused by the F(lp) $\rightarrow$ σ^*(AF) delocalization effects. Also, there is a reduced lp(X)-lp(X) repulsion because of the longer AX bonds and a larger positive charge at A. The bond weakening effects become smaller whereas the polar (ionic) character of the AX bonds increases with increasing fluorination, which always adds to the bond strength of a bond.[89,90]

Second row alternatives. Replacing the N atom with an O atom leads to a decrease in the bond polarity and a smaller change in the charge on the O atom ($+486$ me) when changing from HOH (**28**; O: -895 me) to HOF (**29**; O: -301; F: -142 me) and FOF (**30**; O: $+185$ me; F: -93 me; NBO-CCSD(T) values). Nevertheless, the contraction of the covalent radius of O decreases the OF bond from 1.437 (HOF to 1.407 Å (FOF). The OF bond shortening causes enhanced through-space lp(F)-lp(F) repulsion in FOF, which together with the anomeric delocalization effect lp(F) $\rightarrow$ $\sigma^\star$(OF) (2×10.58 kcal/mol) leads to bond weakening. The latter is documented by the CCSD(T) local OF stretching force constants k^a(OF) (4.326 in HOF; 4.032 mdyn/Å in FOF; BSO values change from 1 to 0.982, Table 1). Again, this indicates a reverse BLBS relationship and an OF bond anomaly. Effects are slightly larger than in the case of the fluoro amine radicals (Fig. 1) because the OF bond is weaker than the NF bond in the amino radicals **2** and **3** and therefore lp-lp repulsion more sensitively registered (see Table 1).

Two remarks are appropriate in connection with the investigation of bonding between strongly electronegative atoms. (i) The calculation of accurate geometries and vibrational frequencies in the case of O-F containing species is a challenge as has been demonstrated by Kraka et al. in the case of FOOF.[91] The CCSD(T)/aug-cc/pVTZ geometries of the current work are in excellent agreement with the available experimental data;[92,93] (**29**: R(OF) = 1.437, experimental value: 1.434 Å; **30**: R(OF) = 1.407, experimental value: 1.403 Å) thus providing evidence that the observed BLBS anomaly for FO bonds is real. (ii) The investigation of triatomic molecules might suggest that the conversion of normal into local modes is not needed to determine the intrinsic bond strengths of these molecules. Empirical bond strength estimates being based on (coupled) normal mode force constants have been suggested. Politzer and Habibollahzadeh[11] derived an empirical bond order n(AB) from the bond length R(AB) and the corresponding normal mode force constant k(AB), which was used for the molecules discussed above. The normal mode decomposition into local modes (see Supporting Information) suggests that mode 1 of **29** has 99.5% OF character, ($\omega_1 = 919$, $\omega_1^a = 920$ cm^{-1}), i.e. any empirical relationship based on the k_1 value will give reasonable results. However, in molecule **30** with its two OF bonds, the asymmetric mode 2 is equally composed of both OF local stretching modes, whereas the symmetric mode 3 is composed of $2\times$ 47.4% local OF stretching and 5.2% FOF bending character. The corresponding normal mode frequencies are $\omega_2(B_2) = 864$ cm^{-1} and $\omega_3(A_1) = 951$ cm^{-1} whereas the true local stretching frequency ω^a(OF) is 888 cm^{-1}, i.e., the kinematically decoupled value is totally different from any of the normal mode frequencies. Therefore, a bond strength relationship based on normal rather than local mode stretching force constants is highly erroneous.

One could expect for FOOF a similar effect as found for FOF, where however, the former has an extremely long OF bond (exp: 1.586;[94,95] MP6/CBS: 1.588; CCSD(T)/CBS: 1.534; CCSD(T)/aug-cc-pVTZ: 1.542 Å).[91] This is a result of a strong anomeric delocalization of the lp(O) electrons into the vicinal $\sigma^\star$(OF) orbitals (delocalization energy: 2×54.82 kcal/mol) thus generating with the longest OF bond also the shortest OO bond of a peroxide (OO: 1.216 Å).[91] Con-

trary to FOF, FOOF follows an inverse BLBS relationship. The long OF bond leads to a CCSD(T) stretching force constant of just 1.825 mdyn/Å, which is in line with the strong anomeric delocalization into the OF bond and its inevitable bond weakening.

Diazenes, Carbenes, Nitrenes, etc. The strongest NF bonds (n range 1.3–1.4, Fig. 1 and Table 1) are found for **23** ($n = 1.312$, R(NF) = 1.318 Å) and **22** ($n = 1.399$, R(NF) = 1.306 Å). Triplet nitrene NF (**23**) is isoelectronic with O_2 and therefore should have significant double bond character (see MO-diagram in Fig. 7). The linear singlet carbene: C=NF (**22**) forms two orthogonal 4π systems with a bonding and nonbonding π MO being occupied (1π and 2π in Fig. 7) thus leading to a formal MO bond order n(MO) of 2 (bond polarities not considered), which has to be compared with a BSO value of 1.399 (Table 1). cis–HN=NF (**24**) and cis–FN=NF (**26**) have longer NF bonds due to increased anomeric delocalization (cis: lp(N) $\rightarrow$ $\sigma^\star$(NF); 26.84 kcal/mol and lp(F) $\rightarrow$ $\sigma^\star$(NN); 11.00 kcal/mol; trans: 8.95 and 14.29 kcal/mol), which causes bond lengthening and weakening. Formaldimine **21** takes an intermediate position (see Fig. 3). For molecules **21** to **27**, a normal inverse BLBS relationship is observed (Fig. 4a) indicating that N-contraction effects caused by just one or two F substituents do not lead to a bond anomaly.

The danger of using BDE values as intrinsic bond strength descriptors

In this work, we have also calculated G4 BDE and BDH(298) values to emphasize the shortcomings of these parameters as reliable descriptors for the intrinsic bond strength. In this connection one has to differentiate between two definitions of what is commonly called bond strength. (i) If one wants to describe fragmentation patterns, e.g., in connection with a mass spectrometry experiment, then BDE values are preferable. The term bond strength is then used as a reaction parameter that includes all changes during the reaction such as bond breaking, rehybridization, electron density reorganization, spin decoupling, energy effects resulting from avoided crossings (in the case of diatomics), Jahn-Teller and pseudo Jahn-Teller effects, new conjugation possibilities in the fragments, etc. (ii) If one wants to describe the strength of the bond as an intrinsic parameter that refers to (i) the equilibrium geometry of a molecule, (ii) is determined by the electronic structure of the molecule, (iii) related to its thermochemical stability, and (iv) provides a means to directly compare bond strengths of different molecules, then the local stretching force constants are preferable. Often BDE values are used as parameters describing the intrinsic bond strength. For example, for the radical fluoro amines, the fluoro amines, and the fluoro oxides, both BDE and BDH values correctly reflect the NF bond anomaly and seem to be suitable to describe the intrinsic bond strength. However, in the case of formaldimine **21**, the carbene **22**, and the nitrene **23** this impression is corrected: BDE values of 68.8, 54.8, 77.6 kcal/mol are in clear contradiction with the BSO values of 0.935, 1.399, 1.312 (Table 1), which has to do with the fact that the dissociation of the N-F bonds in the three molecules leads to totally different stabilization possibilities for the defluorinated fragments. Even more drastic is

the failure of the BDE values as intrinsic bond strength parameters in the case of the fluorinated diazenes. Since a single electron can delocalize in ·N≡N-F thus leading to a relative stable radical, the BDE value for **26** is just 20.6 kcal/mol and by this far below the other calculated BDE values (Table 1).

Often the argument is passed forward that the BDE values might describe at least qualitatively the correct trend of the intrinsic bond strength. However, numerous examples have been shown[35,37–39,46,96] that this hope lacks any quantum mechanical basis and therefore it is always desirable to obtain the intrinsic strength of a bond from vibrational spectroscopy as the local stretching force constants can be always derived.

Conclusions and Outlook

A critical re-evaluation of previously suggested reverse BLBS relationships and the bond anomalies indicated by them, reveals that they are (i) rare and (ii) in most cases relatively small so that high-accuracy quantum chemical calculations as carried out in this work or alternatively spectroscopic investigations in the gas phase are needed to reliably document them. In this work, we have found bond anomalies for (a) fluoro amine radicals, (b) fluoro amines, and (c) fluoro oxides. They do not exist for the equilibrium forms of the higher homologues such as the chloro amines, the fluoro phosphines or the fluoro arsines.

The study of AB bond anomalies requires a suitable bond parameter that reliably reflects any changes in the intrinsic bond strength. This should be preferably a dynamic bond parameter, which probes the strength of the bond for an infinitesimal change in its length. The local stretching force constants derived from the local vibrational modes provide the perfect measure for this purpose as they can be directly derived from either measured or calculated normal mode frequencies.[3,28,29,97]

A reverse BLBS relation always requires two (or more) opposing electronic effects: One, which leads to a bond shortening, and one, which leads to increased bond weakening with decreasing bond length. For the N-F single bonds investigated, the first effect is a decrease in the covalent radius of the central atom due to a strong withdrawal of negative charge as it occurs with increasing fluorine substitution. This of course leads to a contraction of the valence orbitals and subsequently to shorter bonds. For the O-F single bond, the same effect holds, but in general other bond shortening effects can also play a role. We note in this connection that scalar relativistic effects also lead to an orbital contraction and shorter bonds, which in the case of the mercury atom implies a strongly reduced donor ability and weaker bonds as for example documented by the relativistic and non-relativistic bond energies and stretching force constants of HgO and related molecules.[98–100] Hence, other than electron withdrawal effects can lead to shorter bonds in connection with a bond anomaly, but have not been found so far considering that for the HgO example a model BLBS reference in form of a non-measurable non-relativistic bond has to be taken.

Once the bond has been shortened, then anomeric delocalization of the lp(F) electrons into the NF bond and lp(N)-lp(F) or lp(F)-lp(F) repulsion can lead to bond weakening and the observed bond anomaly. As shown for the cases of the planar fluoro amines

and the planar chloro amines, the prediction of a bond anomaly is difficult because of a complex interplay of different reasons: (i) NX bond weakening can be annihilated by electronic effects such as improved pπ-pπ-overlap (in the planar forms), π-delocalization in connection with lp(X) → Ry(A) effects, or a depopulation of the lp(A) orbital (decreasing lp-lp-repulsion). (ii) Alternatively, bond weakening can be enhanced by additional 3s(Cl) → σ^*(AX) delocalization effects as in the case of the planar chloro amines. These additional effects are triggered if bond polarity (determined by effective electronegativities) and electron delocalization complement each other in an effective way. It is easy to predict which molecules should not and which should be prone to bond anomalies. However, for being able to predict that pyramidal chloro amines do not and planar chloro amines do suffer from a bond anomaly a quantitative analysis is needed. It remains as a fact that in any case considered, a reduction of the covalent radius of either central atom or substituent is a prerequisite.

[1] R. M. Badger, *J Chem. Phys.* **1934**, *2*, 128.
[2] R. M. Badger, *J Chem. Phys.* **1935**, *3*, 710.
[3] E. Kraka, J. A. Larsson, D. Cremer, In Computational Spectroscopy: Methods, Experiments and Applications; J. Grunenberg, Ed.; Wiley: New York, **2010**; pp. 105–149.
[4] E. Kurita, H. Matsuura, K. Ohno, *Spectrochim. Acta Part A* **2004**, *60*, 3013.
[5] R. H. Atalla, A. D. Craig, J. A. Gailey, *J. Chem. Phys.* **1966**, *45*, 423.
[6] P. Politzer, *J. Am. Chem. Soc.* **1969**, *91*, 6235.
[7] P. Politzer, J. Timberlake, *J. Org. Chem.* **1972**, *37*, 3557.
[8] P. Politzer, *Inorg. Chem.* **1977**, *16*, 3350.
[9] H. Mack, D. Christen, H. J. Oberhammer, *Mol. Struct.* **1988**, *190*, 215.
[10] D. Christen, O. D. Gupta, J. Kadel, R. L. Kirchmeier, H. G. Mack, H. Oberhammer, J. M. Shreeve, *J Am. Chem. Soc.* **1991**, *113*, 9131.
[11] P. Politzer, D. Habibollahzadeh, *J. Chem. Phys.* **1993**, *98*, 7659.
[12] K. H. Hedberg, K. Obed, E. Robert, J. Kirchmeier, L. Shreeve, *J. Phys. Chem. A* **1998**, *102*, 5106.
[13] M. Kaupp, B. Metz, H. Stoll, *Angew. Chem. Int. Ed. Engl.* **2000**, *39*, 4607.
[14] M. Kaupp, S. Riedel, *Inorg. Chim. Acta* **2004**, *357*, 1865.
[15] J. M. Martell, R. J. Boyd, Z. Shi, *J. Phys. Chem.* **1993**, *97*, 7208.
[16] L. Pierce, N. DiCianni, R. H. Jackson, *J. Chem. Phys.* **1963**, *38*, 730.
[17] H. Kim, E. Pearson, E. H. Appelman, *J. Chem. Phys.* **1972**, *56*, 1.
[18] J. Murrell, S. Carter, I. M. Mills, M. F. Guest, *Mol. Phys.* **1979**, *37*, 1199.
[19] X. H. Ju, Z. Y. Wang, X. F. Yan, H. M. Xiao, *J. Mol. Struct. Theochem.* **2008**, *437*, 95.
[20] R. Harcourt, P. Wolynec, *J. Phys. Chem. A* **2001**, *105*, 4974.
[21] B. A. Lindquist, T. H. Dunning, *J. Phys. Chem. Lett.* **2013**, *4*, 3139.
[22] L. Mueck, *Nat. Chem.* **2013**, *5*, 896.
[23] R. Sanderson, *J. Chem. Educ.* **1976**, *53*, 675.
[24] M. Kaupp, P. vR. Schleyer, *J. Am. Chem. Soc.* **1993**, *115*, 1061.
[25] S. Tang, Y. Fu, Q. Guo, *Acta Chim. Sin.* **2012**, *70*, 1923.

[26] R. D. Ernst, J. W. Freeman, L. Stahl, D. R. Wilson, A. M. Arif, B. Nuber, M. L. Ziegler, *J. Am. Chem. Soc.* **1995**, *117*, 5075.

[27] L. Stahl, R. Ernst, *J. Am. Chem. Soc.* **1987**, *1095*, 5673.

[28] Z. Konkoli, D. Cremer, *Int. J. Quant. Chem.* **1998**, *67*, 1.

[29] D. Cremer, J. A. Larsson, E. Kraka, In Theoretical and Computational Chemistry, Vol. 5, Theoretical Organic Chemistry; C. Parkanyi, Ed.; Elsevier: Amsterdam, **1998**; pp. 259–327.

[30] W. Zou, R. Kalescky, E. Kraka, D. Cremer, *J. Chem. Phys.* **2012**, *137*, 084114.1.

[31] D. Setiawan, E. Kraka, D. Cremer, *J. Phys. Chem. A.* **2015**, *119*, 95441.

[32] R. Kalescky, E. Kraka, D. Cremer, *J. Phys. Chem. A* **2014**, *118*, 223.

[33] W. Zou, R. Kalescky, E. Kraka, D. Cremer, *J. Mol. Model.* **2012**, *19*, 2865.

[34] A. Humason, W. Zou, D. Cremer, *J. Phys. Chem. A* **2014**, *119*, 1666.

[35] R. Kalescky, E. Kraka, D. Cremer, *J. Phys. Chem. A* **2013**, *117*, 8981.

[36] R. Kalescky, E. Kraka, D. Cremer, *Inorg. Chem.* **2014**, *53*, 478.

[37] E. Kraka, D. Cremer, *ChemPhysChem* **2009**, *10*, 686.

[38] R. Kalescky, E. Kraka, D. Cremer, *Int. J. Quant. Chem.* **2014**, *114*, 1060.

[39] R. Kalescky, W. Zou, E. Kraka, D. Cremer, *J. Phys. Chem. A* **2014**, *118*, 1948.

[40] J. Oomens, E. Kraka, M. Nguyen, T. Morton, *J. Phys. Chem. A* **2008**, *112*, 10774.

[41] M. Freindorf, E. Kraka, D. Cremer, *Int. J. Quantum Chem.* **2012**, *112*, 3174.

[42] E. Kraka, M. Freindorf, D. Cremer, *Chirality* **2013**, *25*, 185.

[43] R. Kalescky, W. Zou, E. Kraka, D. Cremer, *Chem. Phys. Lett.* **2012**, *554*, 243.

[44] R. Kalescky, E. Kraka, D. Cremer, *Mol. Phys.* **2013**, *111*, 1497.

[45] D. Setiawan, E. Kraka, D. Cremer, *Chem. Phys. Lett.* **2014**, *614*, 136.

[46] D. Setiawan, E. Kraka, D. Cremer, *J. Phys. Chem. A* **2014**, *119*, 1642.

[47] R. Kalescky, W. Zou, E. Kraka, D. Cremer, *Aust. J. Chem.* **2014**, *67*, 426.

[48] J. Liu, J. Hu, *Future Med. Chem.* **2009**, *1*, 875.

[49] Pollack, P. Fine Chemicals: The Industry and the Business, 2nd ed.; Wiley: New York, **2011**.

[50] K. Raghavachari, G. W. Trucks, J. A. Pople, M. Head-Gordon, *Chem. Phys. Lett.* **1989**, *157*, 479.

[51] D. Woon, T. J. Dunning, *J. Chem. Phys.* **1994**, *100*, 2975.

[52] D. Woon, T. Dunning, *J. Chem. Phys.* **1993**, *98*, 1358.

[53] A. Wilson, D. Woon, K. Peterson, T. Dunning, *J. Chem. Phys.* **1999**, *110*, 7667.

[54] A. D. Becke, *Phys. Rev.* **1988**, *38*, 3098.

[55] C. Lee, W. Yang, R. G. Parr, *Phys. Rev.* **1988**, *B37*, 785.

[56] A. D. Becke, *J Chem. Phys.* **1993**, *98*, 5648.

[57] P. J. Stevens, F. J. Devlin, C. F. Chabalowski, M. J. Frisch, *J. Phys. Chem.* **1994**, *98*, 11623.

[58] V. I. Lebedev, L. Skorokhodov, *Russian Acad. Sci. Dokl. Math.* **1992**, *45*, 587.

[59] J. Gräfenstein, D. Cremer, *J. Chem. Phys.* **2007**, *127*, 164113.

[60] E. B. Wilson, J. C. Decius, P. C. Cross, Molecular Vibrations. The Theory of Infrared and Raman Vibrational Spectra; McGraw-Hill: New York, **1955**.

[61] W. Zou, D. Cremer, *Theor. Chem. Acc.* **2014**, *133*, 1451. 15.

[62] L. A. Curtiss, P. C. Redfern, K. Raghavachari, *J. Chem. Phys.* **2007**, *126*, 084108.

[63] A. Reed, L. Curtiss, F. Weinhold, *Chem. Rev.* **1988**, *88*, 899.

[64] F. Weinhold, C. R. Landis, Valency and Bonding: A Natural Bond Orbital Donor-Acceptor Perspective; Cambridge University Press: Cambridge, **2003**.

[65] C. Glendening, E. D. Landis, F. Weinhold, *J. Comput. Chem.* **2013**, *34*, 1429.

[66] E. Kraka, W. Zou, M. Filatov, J. Gräfenstein, D. Izotov, J. Gauss, Y. He, A. Wu, V. Polo, L. Olsson, Z. Konkoli, Z. He, D. Cremer, COLOGNE15, Dallas, **2015**.

[67] J.F. Stanton, J. Gauss, M.E. Harding, P.G. Szalay with contributions from A.A. Auer, R.J. Bartlett, U. Benedikt, C. Berger, D.E. Bernholdt, Y.J. Bomble, L. Cheng, O. Christiansen, M. Heckert, O. Heun, C. Huber, T.-C. Jagau, D. Jonsson, J. Jusélius, K. Klein, W.J. Lauderdale, D.A. Matthews, T. Metzroth, L.A. Mück, D.P. O'Neill, D.R. Price, E. Prochnow, C. Puzzarini, K. Ruud, F. Schiffmann, W. Schwalbach, C. Simmons, S. Stopkowicz, A. Tajti, J. Vázquez, F. Wang, J.D. Watts, CFOUR. **2010**. Available at: http://www.cfour.de. Last access date: 05/01/2015.

[68] M. Harding, T. Mezroth, J. Gauss, A. Auer, *J. Chem. Theory Comput.* **2008**, *4*, 64.

[69] M. Frisch, et al. Gaussian 09 Revision C.1. Gaussian Inc.: Wallingford, CT, **2010**.

[70] B. Cordero, V. Gomez, A. E. Platero-Prats, M. Reves, J. Echeverroia, E. Cremades, F. Barragan, S. Alvarez, *Dalton Trans.* **2008**, *21*, 2832.

[71] P. Politzer, P. Jin, J. Murray, *J. Chem. Phys.* **2002**, *117*, 8197.

[72] P. Politzer, P. Jin, J. Murray, *J. Comput. Chem.* **2003**, *24*, 505.

[73] D. Khomskii, Transition Metal Compounds; Cambridge University Press: London, **2014**.

[74] R. Pearson, *Chem. Rev.* **1985**, *85*, 41.

[75] I. B. Bersuker, The Jahn-Teller Effect; Cambridge University Press: Cambridge, **2006**.

[76] W. Kutzelnigg, *Angew. Chem. Int. Ed. Engl.* **1984**, *23*, 272.

[77] W. Kutzelnigg, *Theochemistry* **1988**, *169*, 403.

[78] P. Pyykö, *Phys. Scripta* **1979**, *20*, 647.

[79] P. Pyykö, *J. Chem. Res. Synopsis* **1979**, 380.

[80] M. Kaupp, *J. Comp. Chem.* **2006**, *28*, 320.

[81] L. Bartell, *Coord. Chem. Rev.* **2000**, *197*, 37.

[82] P. Schwerdtfeger, P. D. W. Boyd, T. Fischer, P. Hunt, M. Liddell, *J. Am. Chem. Soc.* **1994**, *116*, 9620.

[83] U. Gpik, M. H. L. Pryce, *Proc. R. Soc. Lond. Ser. A* **1957**, *238*, 425.

[84] R. F. W. Bader, *Can. J. Chem.* **1962**, *40*, 1164.

[85] R. G. Pearson, *J. Mol. Struct. Theochem.* **1983**, *103*, 25.

[86] T. A. Albright, J. K. Burdett, M. -H. Whangbo, Orbital Interactions in Chemistry; Wiley: New York, **2013**.

[87] A. L. Allred, E. G. Rochow, *J. Inorg. Chem Nucl. Chem.* **1958**, *5*, 264.

[88] S. S. Zumdahl, Chemical Principles, 5th ed.; Houghton Mifflin Company: Boston, **2005**; pp. 587–590.

[89] L. Pauling, The Nature of the Chemical Bond; Cornell University Press: New York, **1960**.

[90] G. Frenking, S. Shaik, The Chemical Bond; Wiley, **2014**.

[91] E. Kraka, Y. He, D. Cremer, *J. Phys. Chem. A* **2001**, *105*, 3269.

[92] I. Halonen, T. K. Ha, *J. Chem. Phys.* **1988**, *89*, 4885.

[93] Y. Morino, S. Saito, *J. Mol. Spectrosc.* **1966**, *19*, 435.

[94] R. H. Jackson, *J. Chem. Soc.* **1962**, *1962*, 4585.

[95] L. Hedberg, K. Hedberg, P. G. Eller, R. R. Ryan, *Inorg. Chem.* **1988**, *27*, 232.

[96] D. Cremer, A. Wu, A. Larsson, E. Kraka, *J. Mol. Model.* **2000**, *6*, 396.

[97] D. Cremer, E. Kraka, *Curr. Org. Chem.* **2010**, *14*, 1524.

[98] M. Filatov, D. Cremer, *ChemPhysChem* **2004**, *5*, 1547.

[99] D. Cremer, E. Kraka, M. Filatov, *ChemPhysChem* **2008**, *9*, 2510.

[100] E. Kraka, M. Filatov, D. Cremer, *Croat. Chem. Acta* **2009**, *82*, 233.